

Atomically Efficient Synthesis of Self-assembled Monodisperse and Ultrathin Lanthanide Oxychloride Nanoplates

Ya-Ping Du, Ya-Wen Zhang,* Ling-Dong Sun, and Chun-Hua Yan*

Beijing National Laboratory for Molecular Sciences, State Key Laboratory of Rare Earth Materials Chemistry and Applications & PKU-HKU Joint Laboratory in Rare Earth Materials and Bioinorganic Chemistry, Beijing 100871, China

Received December 6, 2008; E-mail: yan@pku.edu.cn; ywzhang@pku.edu.cn

Synthesis of monodisperse colloidal inorganic nanocrystals (NCs) (artificial atoms) and manipulation of their superstructures (super-crystals) have attracted enormous scientific and technological interest in multidisciplinary research fields.¹ So far, thermolysis of single source precursors (SSPs) and its derivatives in surfactant solutions are efficient ways to obtain dimension-tunable (e.g., 0D nanodots, 1D nanowires and nanorods, 2D nanoplates and nanodisks, and 3D nanoflowers) high quality NCs.² With those nanoscale building blocks, complex single-component and multicomponent NC superstructures are assembled either by controlling the dynamic evaporation of NC dispersion in various solvents during the self-assembly process or by isothermally compressing the NC layer at the water subphase.³

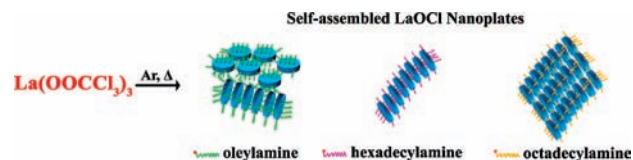
Lanthanide compound NCs such as oxides, sulfides, fluorides, phosphates, and vanadates have received extensive attention due to their unique optical and magnetic properties arising from the 4f electron configuration of the lanthanides.⁴ Although lanthanide oxychlorides (LnOCl) are among this important category of materials, their NCs are scarcely prepared by solution phase syntheses and solid state reactions.⁵

In this communication, we report the synthesis of monodisperse and ultrathin LaOCl nanoplates (ca. 4.0 nm in thickness) via an SSP ($\text{La}(\text{CCl}_3\text{COO})_3$) route (Scheme 1) in long chain amine and 1-octadecene. Depending on the nature of the capping amines, the nanoplates can self-assemble to various superstructures (e.g., single- and multilinear nanoplate arrays).

For a typical synthesis, the slurry of $\text{La}(\text{CCl}_3\text{COO})_3 \cdot \text{H}_2\text{O}$ (1 mmol), oleylamine (OM, 20 mmol), and 1-octadecene (ODE, 20 mmol) in a three-necked flask (100 mL) was heated to 120 °C with vigorous magnetic stirring under vacuum for 30 min in an electromantle, forming a transparent solution. The solution was then heated to 330 °C and maintained for 1 h under Ar. After air cooling, the NCs were precipitated with ethanol, followed by centrifugation and redispersion in cyclohexane.

Transmission electron microscopy (TEM, Philips Tecnai F30 FEG-TEM, 300 kV) reveals the formation of aligned LaOCl nanoplate arrays via the face-to-face and edge-to-edge formation (Figure 1a) when the nanoplates are capped by OM ligands. The nanoplates have a thickness of 3.8 ± 0.2 nm and a diameter of 15.3 ± 0.6 nm for the top (001) surface. Figure 1b shows a typical aligned LaOCl nanoplate (standing on the edge) array along the <001> direction. The interplate distance is ca. 3.3 nm, which roughly fits the thickness of two monolayers of the oleylamine molecules. Determined from high-resolution TEM (HRTEM) images (Figure 1c,d), the nanoplates are single-crystalline with the exposed (110), (101), and (001) planes. They preferably grow along the <110> direction. The spectrum of energy-dispersive X-ray analysis (EDAX) (Figure 1e) confirms the formation of the stoichiometric LaOCl compound (the atomic ratio of La/Cl = 1:1.01). The X-ray diffraction (XRD) pattern and Raman spectrum (Figure S1 in the

Scheme 1. Synthesis Protocol of Self-Assembled LaOCl Nanoplates



Supporting Information (SI)) of the nanoplates demonstrate that the nanoplates are in a PbFCI type structure (tetragonal, space group of $P4/nmm$, JCPDS: 34-1494), with the calculated lattice constants of $a = 0.413$ nm and $c = 0.672$ nm. The (110) reflection has a distinctly narrower peak width than the (003) reflection, indicating the smaller size along the <001> direction. The most intense (110) peak indicates the preferred growth along this plane for the NCs as conforming to the above microscopic analysis.

By changing the hydrocarbon chain of the amines, nanowire-like (Figure 1f) and nanorod-like (Figure 1g) LaOCl nanoplate

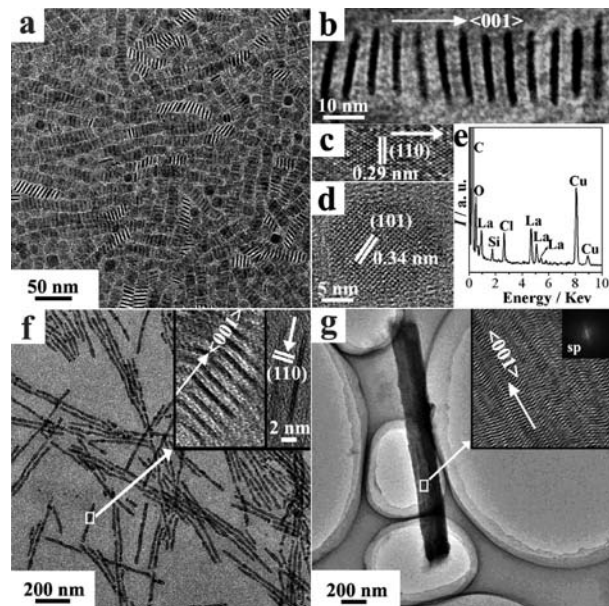


Figure 1. (a) TEM image of oleylamine (OM)-capped LaOCl nanoplate arrays. (b) TEM image of an aligned OM-capped LaOCl nanoplate (standing on the edge) array. (c) HRTEM image of a single OM-capped LaOCl nanoplate standing on the edge. (d) HRTEM image of a single OM-capped LaOCl nanoplate lying flat on the face. (e) EDAX spectrum of the LaOCl nanoplates. (f) TEM and HRTEM (inset) images of nanowire-like LaOCl nanoplate arrays composed of single-linear standing nanoplates capped with hexadecylamine via the face-to-face formation. (g) TEM image of a single nanorod-like LaOCl nanoplate array composed of multilinear standing nanoplates capped with octadecylamine via the face-to-face formation; insets are the HRTEM image of the nanoplate superlattice (SP) and the corresponding FFT pattern.

superstructures of several micron sizes were obtained with hexadecylamine (HDA) and octadecylamine (ODA), respectively. As for HDA, nanowire-like LaOCl nanoplate arrays composed of single-linear standing nanoplates ($(4.2 \pm 0.3) \text{ nm} \times (15.3 \pm 0.6) \text{ nm}$) were obtained via the face-to-face formation along the $\langle 001 \rangle$ direction (Figure 1f and Figure S2 in SI). The nanoplates also grow along the $\langle 110 \rangle$ direction, and the interplate distance is ca. 3.7 nm. The ODA-capped LnOCl nanoplates ($(3.9 \pm 0.3) \text{ nm} \times (12.3 \pm 0.4) \text{ nm}$) formed nanorod-like LaOCl nanoplate arrays (Figure 1g and Figure S3 in SI) composed of multilinear standing nanoplates via the face-to-face formation along the $\langle 001 \rangle$ direction. The fast Fourier transform (FFT) analysis inserted in Figure 1g indicates that the interplate distance is 4.3 nm.

In the present synthesis, the combined use of SSP and mixed solvents seemed to play a key role. Monodisperse LaOCl nanoplates were formed in a mixed solvent of alkylamine and ODE at temperatures beyond 320 °C. The sole use of long chain amine as the solvent yielded soluble but polydisperse and aggregated LaOCl nanoplates (Figure S4 and Table S2 in SI), while the sole use of ODE produced an insoluble solid. LaOCl instead of La_2O_3 was produced from a controlled chlorination of the La–O bond to the La–Cl bond by Cl^- ions produced from the cleavage of the C–Cl bond of the trichloroacetate ligands during the reaction.^{4c} The adoption of some oleic acid in OM and ODE would result in La_2O_3 NCs. The formation of the nanoplate shape for LaOCl is caused by the 2D growth along the $\langle 110 \rangle$ direction with the confined $\{001\}$ planes due to the anisotropic structure of tetragonal LaOCl and its layered structure along the c -axis.^{4c,5a}

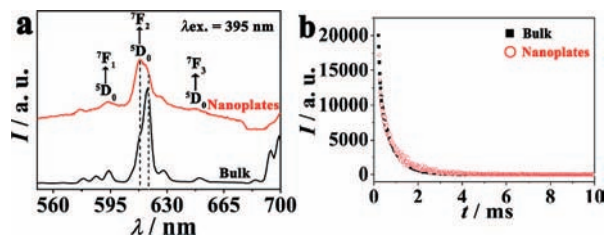


Figure 2. (a) Room temperature photoluminescence spectra of LaOCl/5%Eu nanoplates and its bulk counterpart under $\lambda_{\text{ex}} = 395 \text{ nm}$. (b) Luminescence decay curves of the 613 nm emission of Eu^{3+} ions in the LaOCl/5%Eu nanoplates and its bulk counterpart under $\lambda_{\text{ex}} = 395 \text{ nm}$.

Interestingly, our LaOCl NCs can form diverse self-assembled superstructures regardless of the fabrication conditions (e.g., concentration of NCs dispersion), but strongly depending on the nature of the capped amines used in the NCs synthesis. The OM-capped nanoplates formed nanoarrays via both the face-to-face and edge-to-edge formation (Figure 1a), while the HDA and ODA-capped nanoplates formed single- (Figure 1f) and multilinear (Figure 1g) nanoplate arrays, respectively. The formation of various nanoplate superstructures is considered to arise from the different strengths of the interchain molecular interactions of the capping amine molecules during the self-assembly process of nanoplates under dynamic evaporation of cyclohexane. Under stronger interchain molecular interactions of HDA and ODA, minimization of total energy for the nanoplate micelles led to more compact nanoplate arrays via the face-to-face formation on the TEM grids during the nanoplate deposition.^{1b,3}

Using the present SSP route, we also obtained monodisperse EuOCl ($(4.1 \pm 0.8) \text{ nm} \times (16.3 \pm 0.9) \text{ nm}$) and LaOCl/Eu ($(2.8 \pm 0.3) \text{ nm} \times (12.3 \pm 0.4) \text{ nm}$) nanoplates (Figures S5 and S6 in SI). Figure 2a depicts the emission spectra of the LaOCl/5%Eu nanoplates and its bulk counterpart under $\lambda_{\text{ex}} = 395 \text{ nm}$. The emission spectrum of LaOCl/5%Eu nanoplates was broadened due

to their nanoscale size.⁶ The main emission peaks are ascribed to Eu^{3+} transition from $^5\text{D}_0$ to $^7\text{F}_1$ ($J = 0-3$), and the intensity ratio of $^5\text{D}_0 \rightarrow ^7\text{F}_2$ to $^5\text{D}_0 \rightarrow ^7\text{F}_1$ is equal to the red/orange (R/O) ratio. For the nanoplates, the calculated R/O value is 3.8, distinctly lower than that of the bulk (17.1). The peak intensity ratio of 613 to 618 nm is enhanced with respect to the bulk, suggesting the lower crystal field symmetry for the surface Eu^{3+} ions in the nanoplates.^{6a} The photoluminescent (PL) quantum yields (QYs) (decided by factors such as efficiency of photon absorption and concentration of nonradiative centers for a phosphor)^{5a,6b} of the LaOCl/5%Eu nanoplates is determined to be 2.8%. Figure 2b depicts the luminescence decay curve of the 613 nm emission. The curves can be well fitted into a single exponential function as $I = I_0 \exp(-t/\tau)$ (τ corresponds to Eu^{3+} lifetime). The fitted lifetime is $\tau = 0.75 \text{ ms}$ for the nanoplates, close to that (0.70 ms) for the bulk, meaning the passivation of the nonradiative channels in the nanoplates by the capping ligands.^{6b}

In conclusion, we demonstrate the synthesis of high-quality LaOCl nanoplates via the thermolysis of $\text{La}(\text{CCl}_3\text{COO})_3$ in long chain amine and 1-octadecene. This SSP approach is simple but atomically efficient and has been applied to make monodisperse EuOCl and optically active LaOCl/Eu nanoplates. The uniform amine-capped LaOCl nanoplates can be aligned into nanowire-like and nanorod-like superstructures, as a result of the different strengths of the interchain molecular interactions of the capping molecules during the self-assembly process of the nanoplates. Due to the surface effect, the LaOCl/Eu nanoplates show unique PL properties compared to its bulk counterpart. This work has opened a new window in designing an efficient synthesis protocol for high quality inorganic NCs of a given compound and in controlling their self-assembled superstructures of both theoretical and practical interest. The as-prepared NCs may find use in catalysis, optical nanodevices, and biosensing.

Acknowledgment. We gratefully acknowledge the financial support from the MOST of China (Grant No. 2006CB601104) and NSFC (Grant Nos. 20871006, 20821091, and 20671005).

Supporting Information Available: The synthesis details and more characterization results about the NCs (PDF). This material is available free of charge via the Internet at <http://pubs.acs.org>.

References

- (1) (a) Murray, C. B.; Norris, D. J.; Bawendi, M. G. *J. Am. Chem. Soc.* **1993**, *115*, 8706. (b) Chen, C. C.; Herhold, A. B.; Johnson, C. S.; Alivisatos, A. P. *Science* **1997**, *276*, 398. (c) Rabani, E.; Reichman, D. R.; Geissler, P. L.; Brus, L. E. *Nature* **2003**, *426*, 271. (d) Park, J.; An, K.; Hwang, Y.; Park, J. G.; Noh, H. J.; Kim, J. Y.; Park, J. H.; Hwang, N. M.; Hyeon, T. *Nat. Mater.* **2004**, *3*, 891. (e) Wang, X.; Zhuang, J.; Peng, Q.; Li, Y. D. *Nature* **2005**, *437*, 121.
- (2) (a) Alivisatos, A. P. *Science* **1996**, *271*, 933. (b) Sun, S. H.; Murray, C. B.; Weller, D.; Folks, L.; Moser, A. *Science* **2000**, *287*, 1989. (c) Narayanaswamy, A.; Xu, H. F.; Pradhan, N.; Kim, M.; Peng, X. G. *J. Am. Chem. Soc.* **2006**, *128*, 10310.
- (3) (a) Archibald, D. D.; Mann, S. *Nature* **1993**, *364*, 430. (b) Seo, W. S.; Shim, J. H.; Oh, S. J.; Lee, E. K.; Hur, N. H.; Park, J. T. *J. Am. Chem. Soc.* **2005**, *127*, 6188. (c) Shevchenko, E. V.; Talapin, D. V.; Murray, C. B.; O'Brien, S. *J. Am. Chem. Soc.* **2006**, *128*, 3620. (d) Tao, A. R.; Sinsersuksakul, P.; Yang, P. D. *Nat. Nanotechnol.* **2007**, *2*, 435.
- (4) (a) Cao, Y. C. *J. Am. Chem. Soc.* **2004**, *126*, 7456. (b) Zhao, F.; Yuan, M.; Zhang, W.; Gao, S. *J. Am. Chem. Soc.* **2006**, *128*, 11758. (c) Sun, X.; Zhang, Y. W.; Du, Y. P.; Yan, Z. G.; Si, R.; You, L. P.; Yan, C. H. *Chem.—Eur. J.* **2007**, *13*, 2320. (d) Lehmann, O.; Kömpe, K.; Haase, M. *J. Am. Chem. Soc.* **2004**, *126*, 14935. (e) Stouwdam, J. W.; Raudsepp, M.; van Veggel, F. C. J. M. *Langmuir* **2005**, *21*, 7003.
- (5) (a) Lee, S.-S.; Park, H.-I.; Joh, C.-H.; Byeon, S.-H. *J. Solid State Chem.* **2007**, *180*, 3529. (b) Konishi, T.; Shimizu, M.; Kameyama, Y.; Soga, K. *J. Mater. Sci.: Mater. Electro.* **2007**, *18*, S183.
- (6) (a) Wang, H. Z.; Uehara, M.; Nakamura, H.; Miyazaki, M.; Maeda, H. *Adv. Mater.* **2005**, *17*, 2506. (b) Kömpe, K.; Lehmann, O.; Haase, M. *Chem. Mater.* **2006**, *18*, 4442.

JA8095416